Rev. Roum. Sci. Techn.– Électrotechn. et Énerg.
Vol. **71**, *4*, pp. 543–548, Bucarest, 2026

DUAL-POLARISED CORADIATOR MIMO ANTENNA FOR 5G APPLICATIONS

SRIVIDHYA KRISHNAMURTHY[1], VENMATHI ASIRVATHAM ROHINI [2], VANITHA LINGARAJ[3]

Keywords: Ring with square inclusion; Stepped feed; Multiple input multiple output (MIMO); 5G mobile applications.

Emerging communication systems require effective antenna infrastructure to support the quality of service needed for generation five (5G) mobile networks. A simple, compact, two-element MIMO antenna for future 5G applications is presented in this work. The antenna uses a ring patch with a square inclusion-shaped coradiator design, fed with a stepped microstrip line for 28 GHz operation. The dual orthogonal feeding of the coradiator configures it as a MIMO antenna. The bottom ground plane is altered to form a defected ground, which is further slotted to obtain the required performance. The compact structure of size 20.03x20.03x0.8 mm3 is fabricated on a very popular Rogers 3003 substrate. The antenna offers appropriate gain and antenna efficiency values of 6.3 dBi and 92%, with good diversity behavior, ECC<0.001, suitable for 5G mobile applications.

1. INTRODUCTION

5G enjoys unprecedented development, providing massive connectivity between people and gadgets, enabling remote healthcare, autonomous driving, the Internet of Things, smart cities, local multipoint distribution service (LMDS), and other innovative services. It is also likely that 5G mobile phones may include satellite functionality. Antennas must be flexible to adapt to varied application scenarios [1]. They must support all-band configuration for achieving peak data rate while meeting traffic capacity and mobility requirements, alongside low loss, precise beam coverage, and radiation concentration. The size should be small to be integrated into handheld devices.

Numerous designs are proposed for recent and emerging 5G applications. In [1], a modified and slotted conventional microstrip antenna with a stepped feed is discussed. A half-cut octagonal radiator with a slot, along with partial ground and a stub, is introduced in [2]. The design of a four-element metamaterial-loaded antenna is discussed in [3]. A high eccentric octagonal-shaped radiator with partial ground is offered in [4]. A dual-band multi-element antenna with an offset-fed radiator is tested in [5]. A rectangular slotted radiator with partial ground and unit cell array decoupling is given in [6]. [7] presents an arc-shaped radiating structure.

Fifth-generation communications identify MIMO as one of the prime technologies for its implementation and operation. It forms the backbone of modern communications, well known for its diversity operations, providing reliable, seamless connectivity and promising huge capacity. Compact antenna designs suit handheld applications in modern times. A quad-port antenna with a slotted patch and perforations in the ground is reported in [8]. A many-element, high-isolation MIMO antenna covering the 5G New Radio band is reported in [9]. A boundary-cut square radiator shared by four matched ports with stepped ground is developed in [10].

While prior works have extensively explored conventional multi-element designs, this study focuses on building a concise coradiator MIMO antenna, wherein a single radiator is shared among the multiple ports, achieving high compactness while maintaining sufficient isolation, with a less complex design. Compactness is highly desired in 5G scenarios, which include handheld applications, fixed wireless access, enhanced mobile broadband, UAV detection, automotive monitoring, earth-to-space transmissions, satellite broadband services, air interface design, New Radio (5G NR) communications, the 5G standard on orthogonal frequency division multiplexing, IoT applications, to name a few.

Detailed design of the proposed antenna is discussed in Section 2, followed by Section 3, which provides the discussion on results. Section 4 elaborates on the MIMO performance. Section 5 concludes the work.

2. ANTENNA DESIGN

Circular monopole designs are highly popular due to their simplicity and symmetry in realizing antennas with remarkable performance. They are quite popular in terms of optimizing the radius and feed.

2.1 ANTENNA GEOMETRY

In this paper, a compact MIMO design of dimensions 20.03x20.03x0.8 mm^3 is implemented over a readily available Rogers 3003 substrate with a permittivity of 3 and a loss tangent of 0.0019. The circle-square antenna dimensions seem to suit the mobile handsets used for 5G applications. The elements of the design are isolated by orthogonal feeding and by using a slot in the partial ground plane. Furthermore, the partial ground plane enhances impedance matching by balancing the inductive effect of the radiator against the capacitive effect of the ground. The modified design improves the current distribution on the radiator surface. The combined effect of the ring radiator with truncated and slotted ground, with specialized feeding, helps in greater performance within a smaller volume.

The design thus satisfies the major objectives of compactness, simplicity, and efficient performance over the complex designs of 5G antennas. The proposed design shows striking performance in terms of bandwidth, gain (6.3 dBi), antenna pattern, efficiency 92% and MIMO characterization.

The system design is accomplished as a symmetric two-element coradiator MIMO design with a less complex isolation structure. The dimensions of the prototype antenna are calculated using the following equations. The radius of the circular radiator, R_o is calculated [11] using eq. (1) and the value is found to be 7.499 mm,

$$F = \frac{8.791 \times 10^3}{f_r \sqrt{\varepsilon_r}},$$

$$R_o = \frac{\mathrm{F}}{\sqrt{1 + \frac{2\mathrm{h}}{F\pi\varepsilon_r}\left(\left(\ln\frac{\pi\mathrm{F}}{2\mathrm{h}}\right) + 1.7726\right)}}\ [\mathrm{mm}]. \qquad (1)$$

[1] Sri Venkateswara College of Engineering, Chennai-Bengaluru Highway, Pennalur, India. E-mail: srivi@svce.ac.in
[2] Kings Engineering College, Chennai-Bengaluru Highway, Irungattukottai, India. E-mail: venmathi@kingsedu.ac.in
[3] SA Engineering College, Poonamallee, India. E-mail: vanitha@saec.ac.in

DOI: 10.59277/RRST-EE.2026.4.11

The resonant frequency of the ring antenna is [12],

$$f = \frac{2c}{6.283(R_o + R_i)\sqrt{\varepsilon_{r_{eff}}}},$$

$$\varepsilon_{r_{efr}} = \frac{1}{2}(\varepsilon_r + 1) + \frac{1}{2}(\varepsilon_r - 1)\left(1 + \frac{h}{R_o - R_i}\right)^{-1/2}, \quad (2)$$

where Ro and Ri are the outer and inner radii of the annular ring monopole, ε_r and ε_{reff} are the relative permittivity and effective relative permittivity of the substrate, and h is the height of the substrate. The feedline width is calculated [13] using eq. (3), as W_f= 3.1 mm,

$$W_f = \frac{7.48h}{e^{\left(\frac{50\sqrt{(\varepsilon_r+1.41)}}{87}\right)}} - 1.25t, \quad (3)$$

where W_f is the feed width, and t *is* the thickness of the line.

2.2 EVOLUTION AND OPTIMISATION OF DESIGN

A concise antenna design with amicable MIMO operation is imperative in the recent 5G arena. The prototype antenna is modeled based on the design values. The evolution of the radiator design is shown in Fig.1 (a-d). The coradiator is excited using microstrip feeds of optimized dimensions. Stepped impedance feeding enables 50Ω impedance matching conditions on the structure.

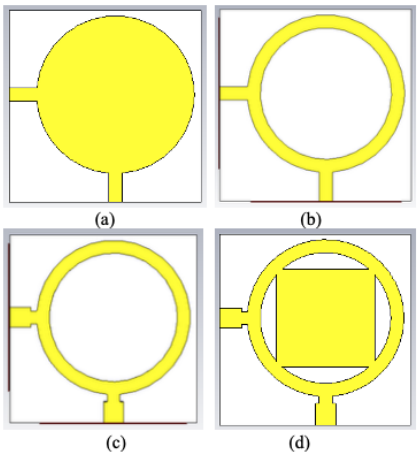


Fig. 1 – Evolution of the antenna radiator.

The ground plane is truncated, and a slot is engraved to obtain impedance matching and isolation, constituting the defected ground structure. A 'defect' so placed disturbs the current distribution and is considered an approximation of an infinite, perfectly conducting current sink [14]. The evolution of the ground plane is shown in Fig. 2.

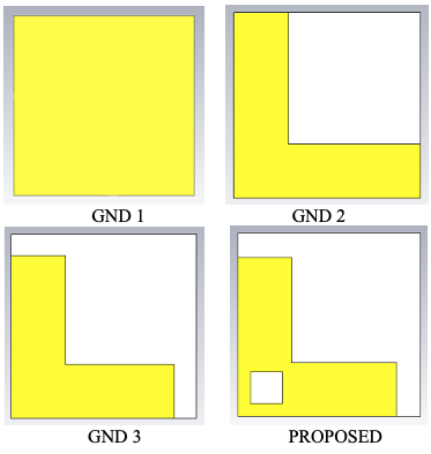


Fig. 2 – Ground plane evolution.

Radiator and ground plane design is critical to derive the required performance of the antenna. The design is studied through surface current concentrations, as in Fig. 3. Complete ground provides an easy path for surface current flow, resulting in the least decoupling. Partial ground shows improvement, but there is no prominent isolation of ports. Optimized ground, as in GND 3, along with a stepped impedance feed, provides superior impedance matching and shows good port decoupling. The inscribed square structure is beneficial for focused radiation, with thorough decorrelation of ports.

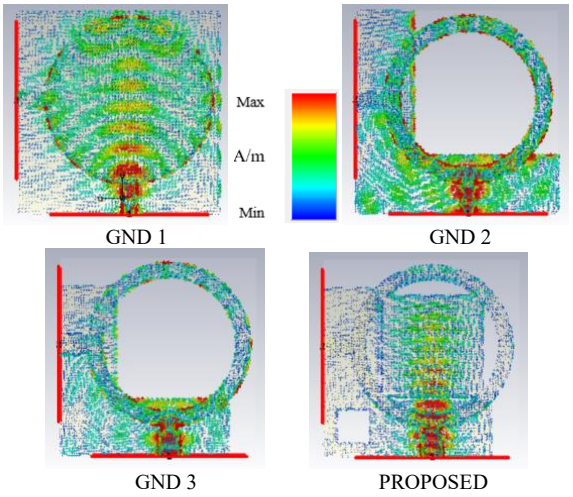


Fig. 3 –Surface current concentration for progressive antenna framework at 28 GHz.

Improvement in the S parameters could be observed with evolving layouts of the ground, as observed in Fig. 4. A shift in resonance and bandwidth is observed with variations in ground length in Fig. 4(a). Additionally, it determines the isolation between antenna elements, as observed in Fig. 4 (b). A slot that is cut out in the disc to develop an annular ring promotes elongation of the current path to provide better impedance matching in the entire resonance band and additionally contributes to miniaturization.

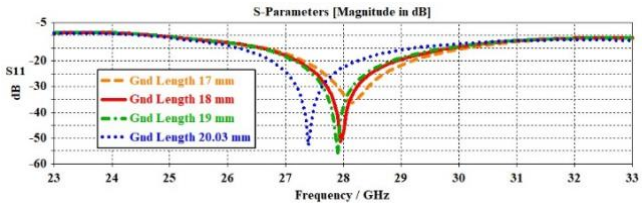


Fig. 4 (a) – Reflection coefficient with ground evolution.

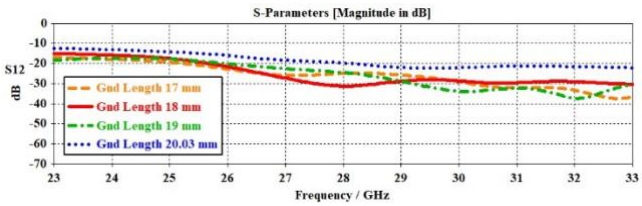


Fig. 4 (b) – Isolation with ground evolution.

The inner and outer radii play a substantial role in influencing the resonant frequency, as observed from Fig. 4(c) and 4(d). They are appropriately chosen to excite the significant modes in the frequency of interest. Inscribing a square structure increases the electrical length of the antenna by providing multiple paths for the current [7]. The length

and width of the feed have a great influence on the resonant frequencies and resonance levels, as shown in Fig. 4(e) and 4(f). Thus, optimization of the antenna layout is performed for parametric cases.

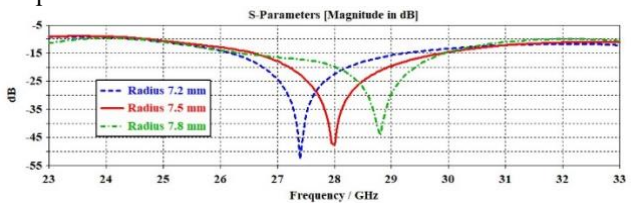


Fig. 4 (c) – Influence of patch radius on Reflection coefficient.

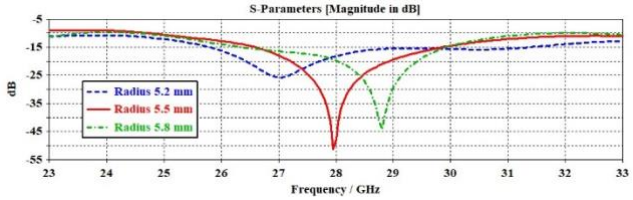


Fig. 4 (d) – Influence of slot radius on Reflection coefficient.

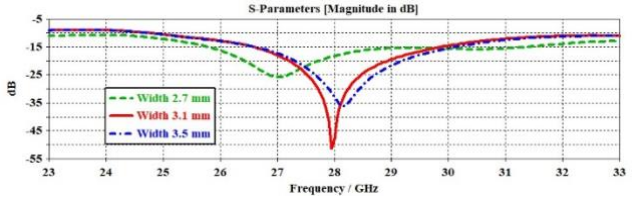


Fig. 4 (e) – Influence of feed width on Reflection coefficient.

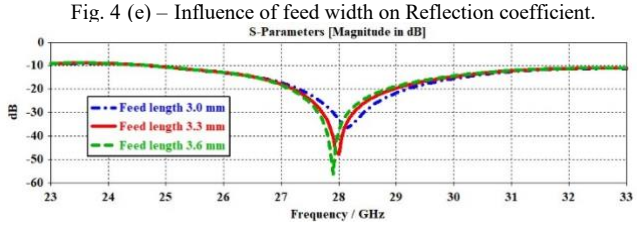


Fig. 4 (f) – Influence of feed length on Reflection coefficient.

Fig. 4 – Improvement in the S-parameters can be observed with evolving ground-plane layouts.

The optimized layout is a MIMO configuration as shown in Fig. 5. The performance of the proposed antenna is as shown in Fig. 6. The reflection coefficient, measured as S_{11} and S_{22} parameters, is as low as -52 dB, as shown in Fig. 6. The decoupling between the elements is significant when MIMO is realized, whereby the elements are proven to be independent of each other. It is measured as S_{21} and S_{12}; the value of -30 dB, regarded as isolation, is evident from the plot in Fig. 6.

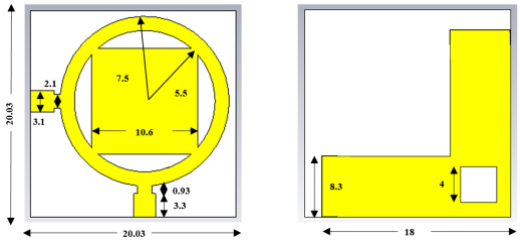


Fig. 5 – Proposed layout (all dimensions in mm).

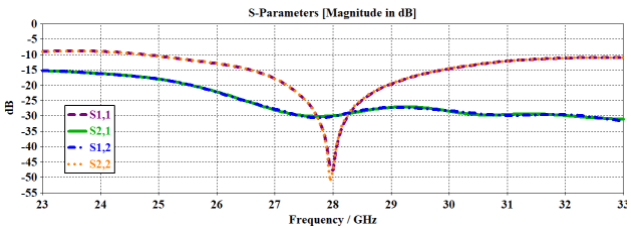


Fig. 6 – S-parameter performance of proposed antenna.

This design allows the antenna to operate with orthogonal polarisations, which doubles the capacity of the channel. The surface current concentration at the center frequency, as in Fig.7, shows that current flows along the X and Y axes while orthogonal ports are excited [10]. Due to the presence of higher-order modes at high frequency, a complex integrated current seems to flow over the radiator surface, still maintaining port-to-port isolation. One can observe that when one port is energized, there is no current flow to the other port, maintaining decorrelation of elements.

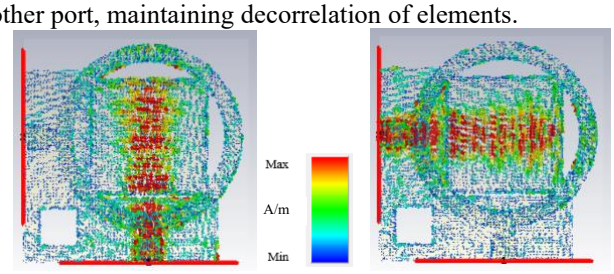


Fig. 7 – Dual polarisation behavior of proposed antenna at 28GHz.

3. RESULTS AND DISCUSSION

The antenna performance is studied and evaluated by analyzing the optimized design in terms of radiation pattern, efficiency, directivity, and gain, resonating at the stipulated 28 GHz. The typical value of VSWR is < 2. The VSWR plot of Fig. 8(a) shows that the antenna is in good agreement in terms of impedance match, with an obtained VSWR value close to 1 at the frequency of interest, while the impedance is 49.4 Ω.

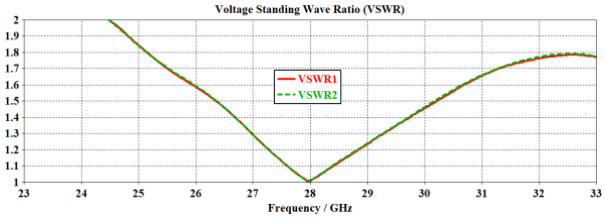


Fig. 8(a) – VSWR performance of proposed antenna.

Gain of an antenna is the "ability to concentrate the radiated power in a given direction or conversely to absorb effectively from that direction". The system shows a good gain value of 6.3 dB at the desired frequency and is stable throughout the band, as shown in Fig. 8(b). Fig. 8 (c) depicts that the antenna radiates with a stable high efficiency of 92%.

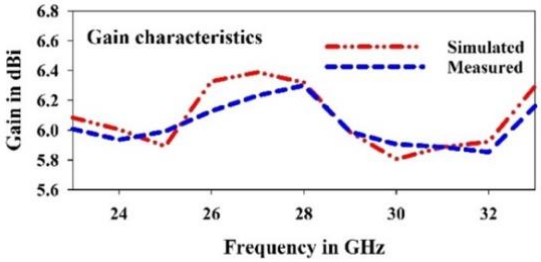


Fig. 8(b) – Gain performance of the proposed antenna.

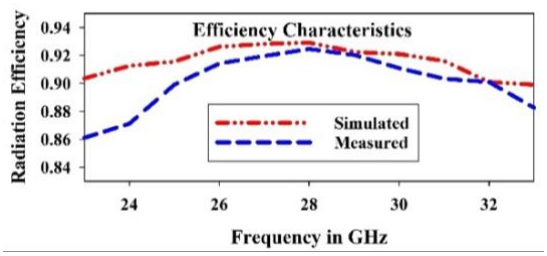
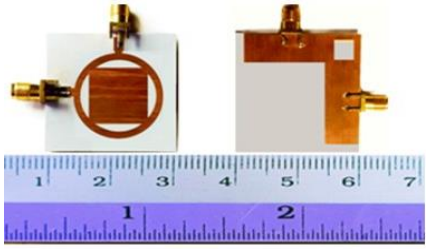


Fig. 8(c) – Efficiency performance of the proposed antenna.

A prototype is developed through a fabrication procedure, as shown in Fig. 9, for validation of the simulations. Measurements are carried out using a Vector Network Analyzer, Rohde & Schwarz model ZVA67, and an anechoic chamber. The resonance performance of the suggested MIMO system is presented in Fig.10. Antenna performance is measured as S_{11} and S_{22} parameters, which show a value as low as -42 dB. Isolation is measured as S_{21} and S_{12}, with a value of -28 dB, as is evident from the above plot. The isolation behavior is stable in the realized band. The measured results seem to align very well with the simulated results.



(a)Front side (b)Back side

Fig. 9 – Fabricated prototype of proposed antenna.

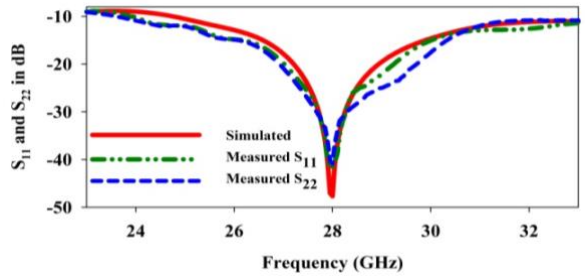


Fig. 10(a) – Reflection coefficient characteristics.

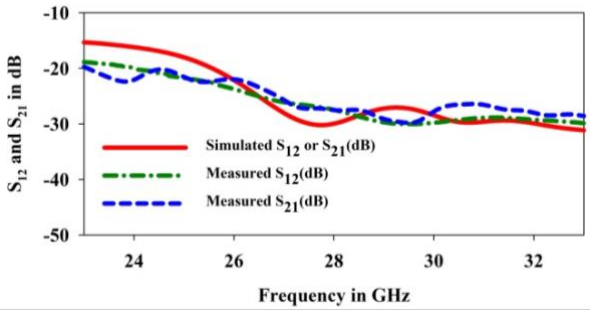


Fig. 10(b) – Isolation characteristics.

The radiation pattern is obtained by measurements in an anechoic chamber, as in Fig. 11. Figure 12 (a-b) shows radiation characteristics of the antenna in a three-dimensional arena. In 2D, simulated and measured values are compared; the pattern orientation clearly shows orthogonal polarisations. Fig.13(a-b) shows co-polarisation and cross-polarisation plots.

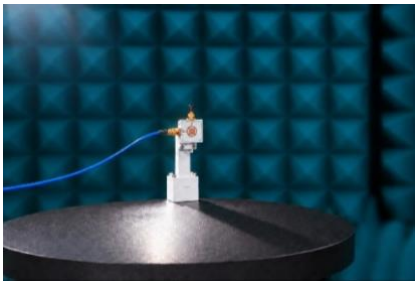
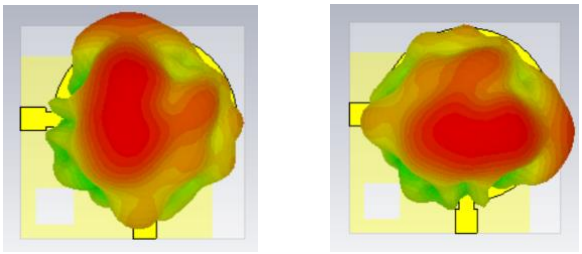


Fig. 11 – Measurement setup in an anechoic chamber.



Port 1 Excitation Port 2 Excitation

Fig. 12(a, b) – 3D Radiation pattern at 28GHz.

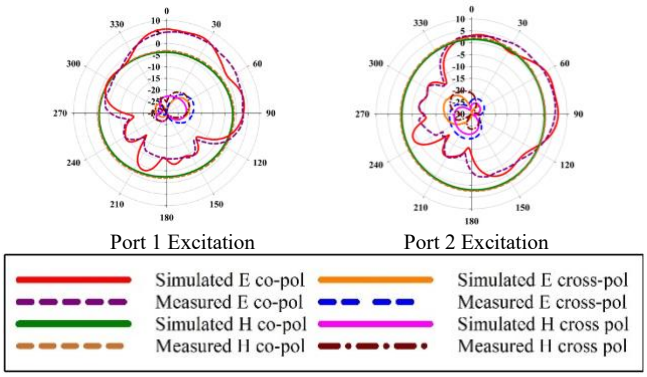


Fig. 13(a, b) – 2D Radiation pattern with co-polarisation and cross-polarisation at 28GHz.

Cross-polarisation discrimination, computed as a ratio of the co-polarised component to the cross-polarised component of a specific polarisation, is high since the difference between co-polar and cross-polar values is higher than 20 dB [15]. Power characteristics: Fig. 14 (a) shows the power distribution of the antenna while the ports are excited. The optimized design converts more of the accepted power to radiated power. With less loss in the patch metallization and dielectric. It is obvious that we get high efficiency.

Channel capacity in communication systems indicates the rate of reliable transmission with minimal errors, of course with noise present. For a Rayleigh fading channel with no line-of-sight and uncorrelated components, capacity is as shown in Fig. 14 (b), calculated using the expression [16],

$$C = N \log_2(1 + SNR)(1 + \rho), \quad (4)$$

where N is the number of antennas, SNR is the signal-to-noise ratio (20 dB), and ρ is the correlation coefficient between the antenna elements. The calculated capacity is 6.645 bps/Hz over the application band, with the ideal value being 7.25 bps/Hz.

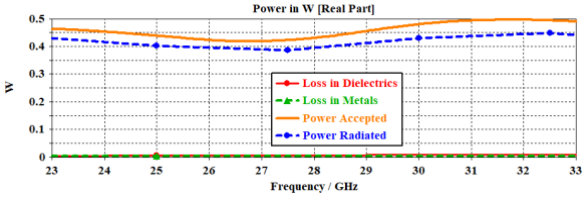


Fig. 14(a) – Power characteristics and component losses.

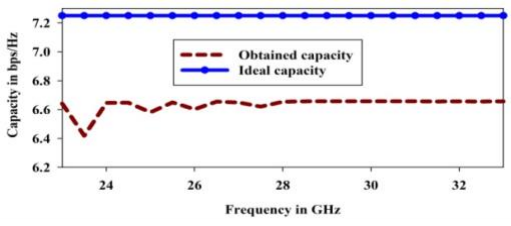


Fig. 14(b) – Calculated capacity of the proposed antenna (bps/Hz).

4. MIMO PERFORMANCE

MIMO antennas improve link reliability, which experiences less fading than a single-antenna system. Hence, data rate and coverage are improved [17], and all the antennas are excited with the same radio transmit power. The MIMO performance of the antenna is analyzed.

Envelope Correlation Coefficient (ECC)

The envelope correlation coefficient characterizes the correlation between any two ports. MIMO antennas should have low ECC to indicate that channels are independent [8]. ECC can be reduced significantly by lowering the mutual coupling. ECC, as per eq. (5) shows a minimal correlation of less than 0.001 in the required band, as in Fig. 15 (a),

$$\rho = \frac{|S_{11} * S_{12} + S_{21} * S_{22}|^2}{(1 - |S_{11}|^2 - |S_{21}|^2)(1 - |S_{22}|^2 - |S_{12}|^2)}. \quad (5)$$

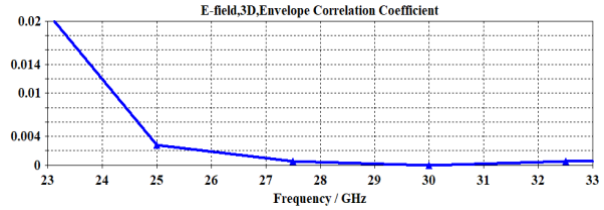


Fig. 15(a) –Envelope Correlation coefficient.

Diversity Gain

The diversity gain essentially measures how much better a communication system performs when diversity techniques are used [8] compared to a system with a single antenna. A value of 9.9dB is obtained, as in Fig. 15(b), upon computing using the eq. (6), against the ideal value of 10 dB [4],

$$DG = 10\sqrt{1 - |\rho|^2}\ [\text{dB}]. \quad (6)$$

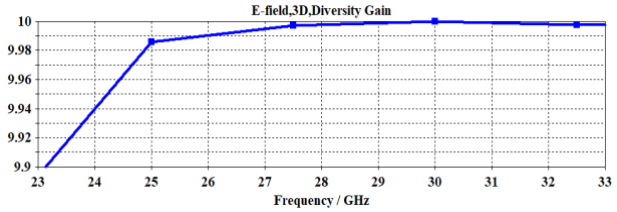


Fig. 15(b) –Diversity Gain (dB).

Mean Effective Gain (MEG)

Mean effective gain quantifies how well an antenna captures and combines the different signal components to maximize the received power in a complex environment [8]. MEG is ideally zero but practically appears lower due to fading. It is given as [4]

$$MEG_i = 0.5\left(1 - \sum_{i=1}^{N} |S_{ij}|^2\right), \quad (7)$$

where *N* is the number of antennas. The value appears to be less than -3 dB, as shown in Fig. 15(c).

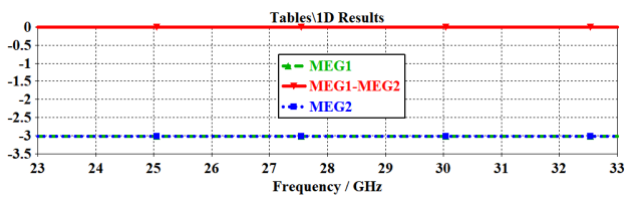


Fig. 15(c) –Mean Effective Gain (dB).

The comparison chart in Table 1 weighs up the performance of the suggested design with related works in the domain. The Coradiator-based design outperforms in terms of design simplicity, compactness, resonant behavior, gain, and efficiency. MIMO properties are also validated.

5. CONCLUSION

A planar, miniaturized, microstrip line-fed MIMO antenna for 5G wireless applications is presented. The designed system resonates at 28GHz, ideal for FSS Earth stations, fixed wireless access services, and mobile services. It also finds use in mobile broadband, ultra-low-latency applications, radar technology, and IoT. In this regard, the narrow beam width associated with antenna elements has led to the use of advanced multiple-input multiple-output (MIMO) architecture. These antenna technologies may be among the key factors for overcoming some of the challenging propagation characteristics of mm-waves and can increase the spectrum efficiency, provide higher data rates, and provide adequate, reasonable coverage. The antenna system offers a good gain of 6.3 dBi and a radiation efficiency of 92%, with desirable reflection and correlation coefficients that are appropriate for 5G communication applications.

CREDIT AUTHORSHIP CONTRIBUTION

All authors contributed to the study conception and design.
All authors read and approved the final manuscript.

Received on 18 January 2026

REFERENCES

1. R.R. Elsharkawy, K.F.A. Hussein, A.E. Farahat, “Circularly-polarized 28-GHz antenna for next generations of communication systems,” Scientific Reports, **15**, Art. no. 5745 (2025).
2. P. Tiwari, M.K. Gaur, M. Kaushik, A. Shastri, B. Singh, V. Gahlaut, “Performance evaluation of wideband dual-port octagonal-shaped millimeter-wave MIMO antenna for satellite communication,” International Journal of RF and Microwave Computer-Aided Engineering, **2025**, 14 pages, Art. no. 1456913 (2025).
3. M.A. Rahman et al., “Metamaterial-based tri-band compact MIMO antenna system for 5G IoT applications with machine learning performance verification,” Scientific Reports, **15**, Art. no. 22866 (2025).
4. M. Soman, P. Kumar, M. Sharma, “Design and testing of a novel MIMO antenna for the 28 GHz millimeter wave band,” Journal of Information Systems Engineering and Management, **10**, *53*, pp. 164–179 (2025).
5. W.T. Sethi et al., “Pattern diversity-based four-element dual-band MIMO patch antenna for 5G mm-wave communication networks,” Journal of Infrared, Millimeter, and Terahertz Waves, **45**, pp. 521–537 (2024).
6. D. Khan, A. Ahmad, D.Y. Choi, “Dual-band 5G MIMO antenna with enhanced coupling reduction using metamaterials,” Scientific Reports, **24**, Art. no. 96 (2024).
7. P. Kumar et al., “An ultra-compact 28 GHz arc-shaped millimeter-wave antenna for 5G application,” Micromachines, **14**, *5* (2023).
8. N.E. Nasri, M.E. Ghzaoui, M. Fattah, “A quad port MIMO antenna with improved bandwidth and high gain for 38GHz 5G applications,” Franklin Open, **6**, Art. no. 100078 (2024).
9. Z. Wang, W. You, M. Yang, W. Nie, W. Mu, “Design of MIMO antenna with double L-shaped structure for 5G NR,” Symmetry, **15**, *3* (2023).
10. L. Malviya, S. Chouhan, “Multi-cut four-port shared radiator with stepped ground and diversity effects for WLAN application,” International Journal of Microwave and Wireless Technologies, **11**, pp. 1044–1053 (2019).
11. I.U. Din et al., “Frequency-selective surface-based MIMO antenna array for 5G millimeter-wave applications,” Sensors, **23**, Art. no. 7009 (2023).
12. P.R. Meher, S.K. Mishra, “Design and development of mathematical equivalent circuit model of broadband circularly polarized semi-

annular ring-shaped monopole antenna," Progress in Electromagnetics Research C, **129**, pp. 73–87 (2023).
13. M. Munde, A. Nandgaonkar, S.B. Deosarkar, "Dual feed wideband annular ring microstrip antenna with circular DGS for reduced SAR," Progress in Electromagnetics Research B, **88**, pp. 175–195 (2020).
14. M.K. Khandelwal, B.K. Kanaujia, S. Kumar, "Defected ground structure: fundamentals, analysis, and applications in modern wireless trends," International Journal of Antennas and Propagation, **2017**, 22 pages, Art. no. 2018527 (2017).
15. P. Jha, A. Kumar, N. Sharma, "A metamaterial-inspired split-ring resonator accomplished multiband antenna for 5G and other wireless applications," Rev. Roum. Sci. Techn. – Électrotechn. Et Énerg., **68**, *2*, pp. 127–131 (2023).
16. R.N. Tiwari, D. Sharma, P. Singh, P. Kumar, "A flexible dual-band 4 × 4 MIMO antenna for 5G mm-wave 28/38 GHz wearable applications," Scientific Reports, **14**, Art. no. 14324 (2024).
17. P. Ramesh et al., "Performance analysis of channel modeling for 5G networks," in IEEE International Conference on Next Generation Electronics (2026).
18. M.M. Basha, P. Pradeep, S. Gundala, J. Syed, "Design of compact and high gain dual-band four-port MIMO antenna array for mm-wave 5G communications," Results in Engineering, **25**, Art. no. 104153 (2025).
19. M. Sharma, B.R. Perli, L. Matta, T. Addepalli, K. Sharma, F.N. Sibai, "Flexible four-port MIMO antenna for 5G NR-FR2 tri-band mm-wave application with SAR analysis," Scientific Reports, **14**, Art. no. 29100 (2024).
20. A.A. Megahed, E.H. Abdelhay, M. Abdelazim, H.Y.M. Soliman, "5G millimeter wave wideband MIMO antenna arrays with high isolation," Journal of Wireless Communication Networks, **2023**, *61* (2023).
21. W.A.E. Ali, A.A. Ibrahim, A.E. Ahmed, "Dual-band millimeter wave 2 × 2 MIMO slot antenna with low mutual coupling for 5G networks," Wireless Personal Communications, **129**, pp. 2959–2976 (2023).

Table 1

Performance comparison with recent state-of-the-art in the literature.

Author (Year)	Type of antenna	Design Complexity	Design Parameters	Measurements	Applications
Poonam Tiwari (2025) [2]	Octagonal patch with diamond slot and I stub in ground	Design: Complex No of Elements: 2	Res Freq:25-35 GHz Dimension: 31×18×1.6 mm^3 2.9λ × 1.68λ	Isolation:24 dB Gain:6.46 dBi Efficiency: 95% ECC:<0.0007	Small satellite systems
Daud Khan (2024) [6]	Slotted conventional patch alongside a metamaterial layer and partial ground	Design: Complex No of Elements: 2	Res Freq:24.8-28.6 GHz Dimension: 18×9.2×0.787 mm^3 1.68λ × 0.859λ	Isolation:22 dB Gain:6 dBi Efficiency: 89% ECC:0.0001	Millimeter wave 5G cellular applications
Iftikhar Ud Din (2023) [11]	Modified FSS based semicircular slot cut radiator with ground slot	Design: Complex No of Elements: 2	Res Freq:27.2-28.8 GHz Dimension: 18×19×0.8 mm^3 1.68λ × 1.69λ	Isolation:26 dB Gain:7.2 dBi Efficiency: 86% ECC:0.002	Video streaming communication applications
Mahaboob Basha (2025) [18]	U shaped slotted rectangular patch antenna with slotted ground	Design: Complex No of Elements: 2	Res Freq:27.2-28.7 GHz Dimension: 21.8x10.4x0.79 mm^3 2.03 λ × 0.97λ	Isolation: 26 dB Gain:7.5 dBi Efficiency: 90% ECC:0.002	5G mm-wave applications
Manish Sharma (2024) [19]	Loop like microstrip radiator with parasitic elements	Design: Complex No of Elements: 2	Res Freq: 27.7–28.1 GHz Dimension: 31×19×0.4 mm^3 2.89λ × 1.77λ	Isolation:16 dB Gain:5.8 dBi Efficiency:89% ECC:0.004	High density fixed services, Radio navigation services (RNS)
Amany A. Megahed (2023) [20]	Circle modified as tree like radiator with slotted stub between elements	Design: Complex No of Elements: 2	Res Freq: 27-40 GHz Dimension: 55.27×27.63×1.6 mm^3 5.16λ × 2.58λ	Isolation: 23 dB Gain:5.5 dBi Efficiency:79% ECC:0.002	5G mm-wave applications
Wael A. E. Ali (2023) [21]	Crescent shaped loaded with stub with slotted ground	Design: Moderate No of Elements: 2	Res Freq: 25.5-30.5 GHz Dimension: 30×15×0.203 mm^3 2.8λ × 1.4λ	Isolation: 32 dB Gain:5.5-6 dBi Efficiency: 86% ECC:0.0001	5G wireless tele-communication applications
Proposed	**Square inscribed ring coradiator with stepped feed and slotted partial ground**	**Design: Simple No of Elements: 2**	**Res Freq:25-32 GHz Dimension: 20.03×20.03×0.8 mm^3 1.87λ × 1.87λ**	**Isolation:30 dB Gain:6.3 dBi Efficiency: 92% ECC:<0.001**	**FSS Earth stations, Fixed wireless access services**